Elliptic Aperture Coaxial Sensor

Mabrouka Haiba A. Ehtaiba

Faculty of Engineering, Electrical and Electronics Department, Sirte University, Sirte, Libya
Corresponding Author: ehtaiba.m@su.edu.ly

ARTICLE INFO

ABSTRACT

Flat open-ended coaxial sensors are increasingly popular for numerous measurement techniques, as a non-destructive method, due to the increased sensitivity and contrast obtained at microwave frequencies. The flat aperture of the sensor limits the practical application of such a method, particularly in diagnosis. In this paper, an elliptic aperture coaxial sensor with small dimensions is introduced and numerically analysed. Using finite element method, the radiation from the elliptical aperture into a two-layer dielectric medium is examined. Explicit contrast of reflection coefficient in both magnitude and phase, and high sensing depth are obtained with such a sensor aperture at low microwave frequencies of 0.1, 0.3, 1, and 3 GHz.

1. Introduction

Among several methods, microwave sensors have now found wide use in many applications based on the use of contrast in dielectric properties between different materials [1]. This gives assurance of early detection and the practical usefulness of the developed system [2]. Whereas flat aperture coaxial sensors are not capable of penetrating easily into semi-solid and a multi-layered material (i.e., a stratified medium), elliptical aperture sensors developed to permit non-destructive measurement of such materials, with the advantage of having higher sensitivity at low frequencies than the flat aperture probes. To achieve high accuracy and sensitivity at lower microwave frequencies (for example, the 0.1 to 3 GHz range used

here), the aperture of the sensors should have a large sensing area. The use of a sharp aperture maximizes this sensing area whilst keeping the diameter of the coaxial cable small. The large sensing area means that the sample covering factor will be high (i.e., a high fraction of the electric field energy will be exposed to the sample), so the sensor will be more sensitive to the presence of the sample. High sensing area can be accomplished using elliptic apertures with high cut angles (φ), but this also necessitates a large sample size.

In 1992, Ghannouchi et al. [3], have introduced different open-ended elliptical apertures, so called needle-type coaxial probes [4], for measurement of microwave permittivity of methanol and demonstrated increased sensitivity in the low microwave frequency range from 2 to 4 GHz. The study was done by Ghannouchi et al., [3] shown that open-ended elliptical coaxial probes (bevelled probes) can be successfully used in wideband dielectric constant measurements with the advantages of increasing sensitivity and can easily be applied to gels and living tissues, and in general for biological applications both for measurements and microwave radiation treatment.

Previously, many sensor types based on the reflection coefficient have been fabricated, which are highly sensitive to the presence of the dielectric properties of the high-permittivity liquids or human tissue [5]. However, these sensors have limited accuracy, particularly with low permittivity values [6]. For example, a flanged coaxial probe with larger dimensions radiating into a material was presented in [7]. This was used for achieving high sensitivity to measure materials with a low dielectric constant at low microwave frequencies, since no distinction can be made between the phase and amplitude characteristics of the reflection coefficient for different values of the dielectric constant with probes of small dimensions. It is thus clearly proven that a probe with larger dimensions drastically improves measurement accuracy for low permittivity materials at frequencies up to 1.5 GHz.

In this paper, small dimensions elliptic aperture sensors are introduced to investigate the sensing depth with a two-layer sample with different properties at low microwave frequencies 0.1-3 GHz.

2. Sensor Modelling

In 1991, Gabriel showed that the finite element method (FEM) is well suited to the study of the fringing fields of coaxial probes [8]. For this reason, the FEM was chosen to analyse the electromagnetic field distribution around the sensor aperture by using Electromagnetic Professional (EMPro) simulator. In this paper, the application of FEM in EMPro was extended to the determination of reflection coefficient of air and different samples by using two different elliptic aperture coaxial sensors as illustrated in Figure 1.
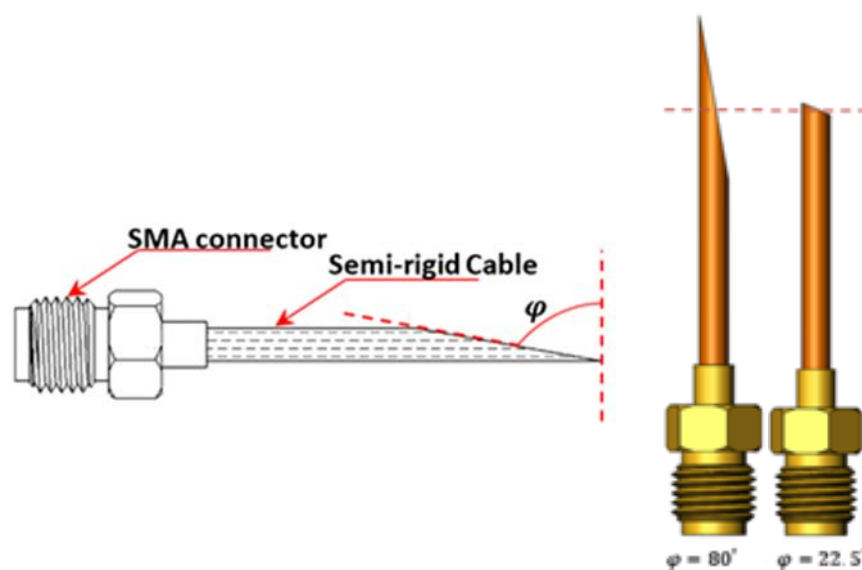

Figure 1: Open-ended coaxial sensors with different apertures.

The open-ended coaxial sensor used in this paper has an inner radius, 0.255 mm and an outer radius, 0.84 mm. The inner of the coaxial line is made of copper, surrounded by PTFE or Teflon (ε_r=2.05) as a dielectric, while the external medium of the coaxial aperture sensor is air (ε_r=1) or a lossy material. All conductors of coaxial probe are assumed perfect electric conductor (PEC). Consequently, the continuity boundary conditions for tangential component of the electric field are applied and imposed at a border of conductors. An electromagnetic wave having its direction of propagation along the coaxial cable is introduced, imposing port type boundary conditions on the one end of the cylinder that models the coaxial probe. On the input port an excitation wave is imposed having an incident power of 1 mw. At the outer boundary, the continuity boundary condition (PEC) sets the tangential component of the electric field, E_z to zero. Generally, the low reflecting or so-called radiation boundary is based on the difference between the total field and the field of the incident wave.

The sensor is immersed into the material to be tested. Then, the waves scattered from the sensor aperture would penetrate into the target sample which entirely covers the aperture area of sensor. The electromagnetic field distribution in the vicinity of the aperture is determined, on the basis of aperture theory and boundary matching of the field components which are results of the solution to a boundary value problem. A solution of the scattering from the flat open end of a coaxial line in contact with a lossy dielectric was presented by Mosig [9]. The formal analysis solution of the boundary-value problem was introduced by King and Wiltse in 1961 [10] for the case of an elliptic coaxial line filled with isotropic dielectric material. The dielectric properties of the material determine the measured quantities such as complex reflection coefficient at the aperture. This reflection coefficient originates from transmission-line theory and is defined in terms of a transmitted and reflected electric field which is formulated in terms of complex-valued, frequency dependent matrices.

3. Simulation Performance

The technique is based on calculating reflection coefficients using EMPro software, which their values depend on the operating frequency, sensor aperture geometry, and the dielectric properties of the sample under test. An open-ended coaxial cable with two cut angles is adopted for the design of the sensors (i.e., $\varphi = 22.5°$ and $\varphi = 80°$ degrees). Several types of samples are tested to verify sensor performance over the frequency range 0.1 GHz to 3 GHz. Standard (i.e., flat) aperture sensors cannot penetrate tissue when made from semi-rigid cables, unlike that for the needle sensor. A major electrical difference between the two structures is that the needle-type sensor has a much larger sensing region, which is ellipsoidal. The radiated energy density is greatest near the aperture and decreases monotonically in the radial direction. Therefore, as with the open-ended coaxial sensor, materials closer to the aperture have more impact on the sensed reflection values.

The simulation process uses the mesh pattern, and the electric fields in the design are calculated. S-parameters are then computed based on the electric fields. If the adaptive frequency sample sweep type is chosen, fast and accurate simulation is generated, based on a rational fit model. The wave equation as expressed in Eq. (1) is solved by EMPro to calculate the full 3D field solution [11].

$$\nabla \times \left(\frac{1}{\mu_r} \nabla \times E(x, y, z) \right) - k_o^2 \varepsilon_{rc} E = 0 \tag{1}$$

where μ_r is the complex relative permeability, ε_{rc} is the complex relative permittivity, $E(x,y,z)$ is a complex vector representing an oscillating electric field and k_o is the free space phase constant ($k_o{}^2 = \omega^2 \mu_o \varepsilon_o$).

For excitation, a wave with unit amplitude at broadband frequencies (0.1 to 3 GHz) is applied between the inner- and outer-conductor of the sensor. The incident wave which propagates to the sensor surface was made by exciting E_ρ and H_ϕ on the line of length L=20 mm. The three-dimensional electromagnetic structure of the elliptical-aperture coaxial sensor shown in Figure 2 is considered. The results computed by EMPro are illustrated in the next section for different dielectric materials.
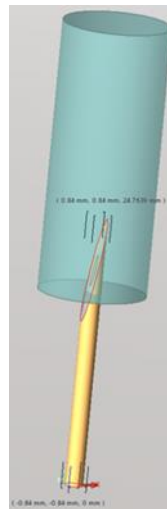

Figure 1: The three-dimensional electromagnetic structure of the elliptical aperture.

3.1   *Frequency effect examination*

Numerically, methanol sample was accurately represented by the Debye equation as expressed in Eq. (2). Methanol was used because its dielectric properties are well-known and high chemical purity samples are easily obtainable. The elliptic aperture of each sensor was entirely immersed into the methanol sample to examine the frequency effect on the reflection coefficient values.

$$\varepsilon^* = \varepsilon_\infty + \frac{\varepsilon_s - \varepsilon_\infty}{1 + j\omega\tau} \tag{2}$$

where the Debye parameters of methanol are static dielectric constant ε_s = 34.8, high dielectric constant ε_∞ = 4.5, characteristic relaxation time τ = 56 ps, and ω is the angular frequency [12].

3.2   *Sensitivity examination with distance sweep*

A two-layer dielectric medium was assumed to have a real permittivity. The first layer has ε_r = 1 and the second one has ε_r = 10. The aperture of φ = 22.5° sensor was set 1mm distance away from the interface line between the two layers, after that, the

distance sweep has carried out at constant frequency values of 0.1, 0.3, 1, and 3 GHz. Furthermore, to precisely examine the sensitivity in terms of permittivity, distance sweep of a two-layer lossy sample of fat and muscle tissues was carried out with both sensors.

4. Results and Discussion

A three-dimensional geometry of two elliptic aperture sensors was implemented in EMPro for a detailed examination of the ability to distinguish the effect of the contrast in dielectric properties on the calculated reflection coefficients. Different configurations of the sensitivity test as a function of microwave frequency, cut angle of sensor aperture, and permittivity are accomplished numerically.

The sensitivity of both sensors was examined with air and then methanol to determine the relative complex reflection coefficient of methanol. For $\varphi = 22.5°$ and $\varphi = 80°$ sensors, it is clear that as frequency increases from 0.1 GHz to 3 GHz, the relative complex reflection coefficient of methanol decreases in magnitude $|S_{11}|$ and increases in phase as illustrated in Figure 3 (a) and Figure 3 (b) respectively. Worthwhile improvements in performance for the sharpest aperture sensor, the magnitude and phase values of relative complex reflection coefficient have significant contrast at 3 GHz.
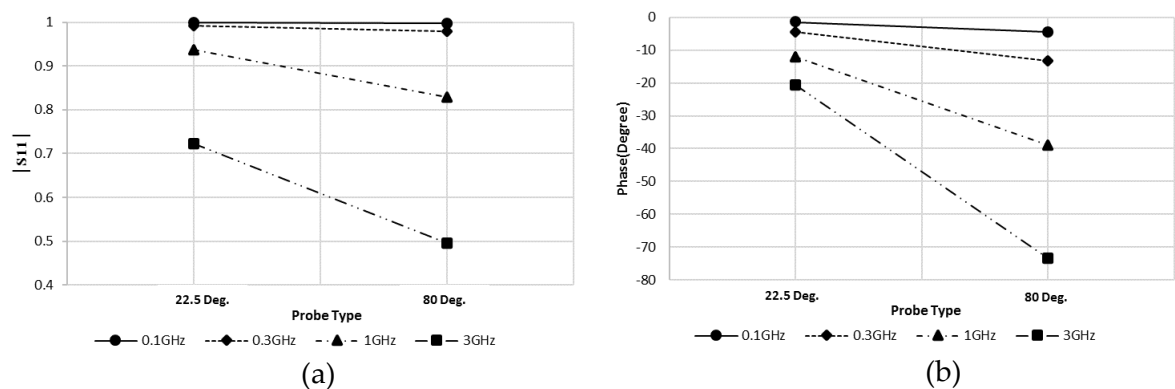

Figure 2: Relative reflection coefficient of methanol, (a) Magnitude, (b) Phase.

Results are given in Figure 4 and Figure 5 shows a numerical distance sweep with a step of 10 μm and a total sweep distance of 2 mm for $\varphi = 22.5°$ and 5 mm for $\varphi = 80°$ sensors, to assess the degree to which each sensor is able to detect different samples.

In Figure 4, the medium in contact with the sensor was assumed a two-layer dielectric medium. The $\varphi = 22.5°$ sensor tip was immersed into the first layer of $\varepsilon_r = 1$ and set 1 mm away from the second layer of $\varepsilon_r = 10$. The magnitude $|S_{11}|$ of reflection coefficient plotted as a function of εr and distance sweep is illustrated in Figure 4 for $\varphi = 22.5°$ sensor at 0.1, 0.3, 1, and 3 GHz. Followed by a plot of the phase

of the reflection coefficient as illustrated in Figure 5 (a) at 0.1 GHz and 1 GHz and Figure 5 (b) at 0.3 GHz and 3 GHz. The magnitude decreases dramatically as frequency increases with obvious contrast. The phase comparison has demonstrated a great increase in phase contrast when frequency increases by ratio of 10.
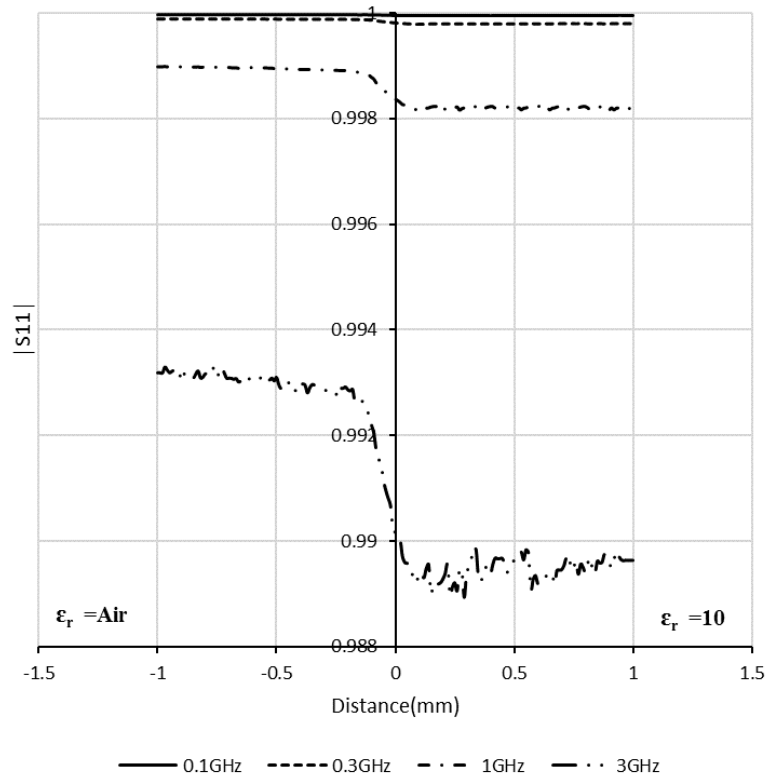

Figure 3: Magnitude of reflection coefficient of φ=22.5° sensor with distance and frequency for ε_r = 1 and 10.
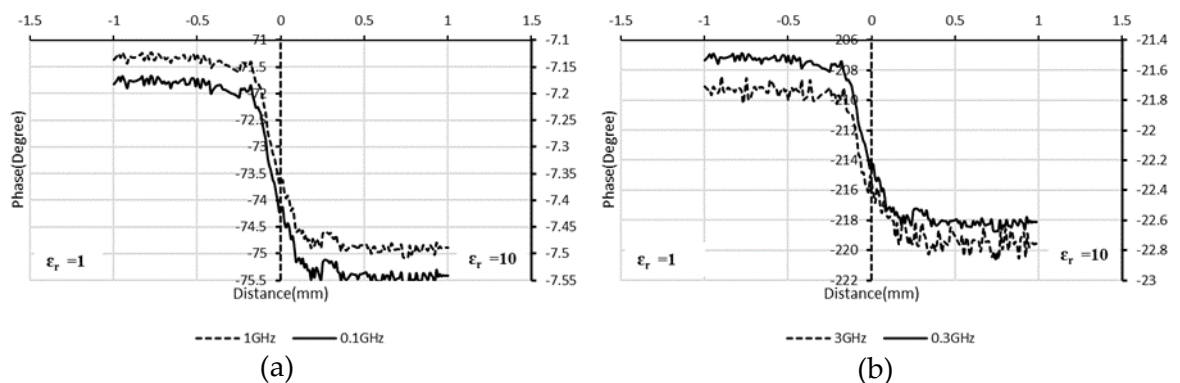

(a)   (b)

Figure 4: Phase of reflection coefficient of φ=22.5° sensor with distance for ε_r = 1 and 10, at (a) 0.1 GHz and 1 GHz, (b) 0.3 GHz and 3 GHz.

To investigate the sensing depth of each sensor with lossy material, two phantoms of human tissues were represented by Debye model. The same distance sweep was used to generate the same plots for different elliptical apertures with fat and muscle tissues at 0.1, 0.3, 1, and 3 GHz. $|S_{11}|$ and phase of φ = 22.5°sensor are illustrated in

Figures 6 and Figure 7 respectively. As a result of increasing the frequency, the relative sensitivity noticeably enhanced, as indicated in Table 1.
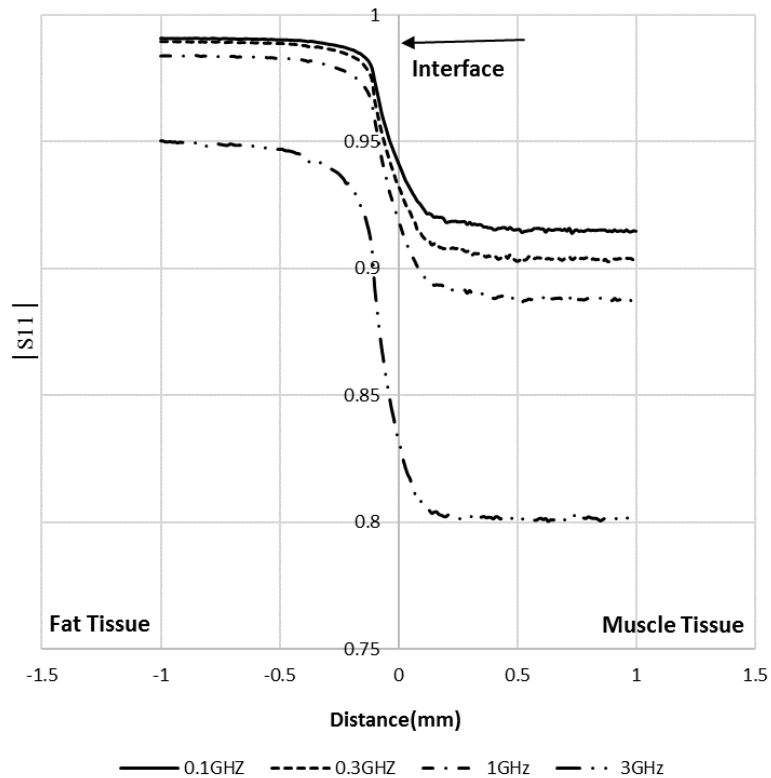

Figure 5: Magnitude of Reflection Coefficient of φ=22.5° sensor with distance and frequency for Fat and Muscle tissues.
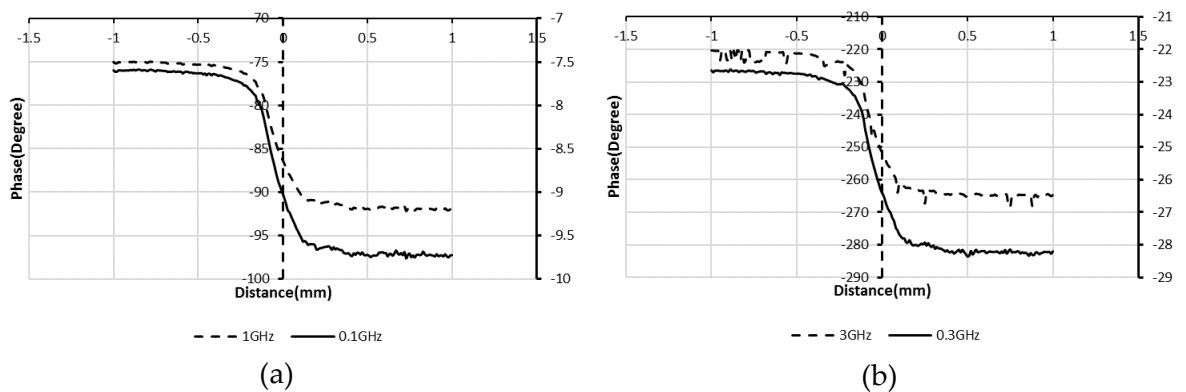

(a)   (b)

Figure 6: Phase of Reflection Coefficient of φ=22.5° sensor with distance for Fat and Muscle tissues, at (a) 0.1 GHz and 1 GHz, (b) 0.3 GHz and 3 GHz.

Table 1. Relative sensitivity percentage of φ=22.5°, at 0.3, 1, and 3 GHz.

$\varphi = 22.5°, f = 0.1\ GHz\ as\ reference$						
$f(GHz)$	$f = 0.3GHz$		$f = 1GHz$		$f = 3GHz$	
	$\|S_{11}\|$ %	*Phase* %	$\|S_{11}\|$ %	*Phase* %	$\|S_{11}\|$ %	*Phase* %
Fat	0.17	198.22	0.72	887.5	4.19	2839.83
Muscle	1.08	189.28	2.99	845.03	12.33	2615.32

Fat and muscle layered-sample distance sweep for phase of reflection coefficient are illustrated in Figure 7 (a) at 0.1 GHz and 1 GHz, and Figure 7 (b) at 0.3 GHz and 3 GHz respectively. It has been found that the sensor was more sensitive for complex reflection coefficient measurements of high loss media such as muscle. In addition, to investigate the sensing depth as the aperture cut angle increases from 22.5° to 80°, a comparison was made between the two apertures at 0.1 GHz and 1 GHz as illustrated in Figure 8 and Figure 9. Obvious difference yielded by magnitude │S₁₁│ and phase as illustrated in Figure 8 and Figure 9, (a) at 0.1 GHz, and (b) at 1 GHz respectively.

From the results of both frequencies, the values obtained for the magnitude and phase of the reflection coefficient with varying permittivity validate the theory for the open-ended coaxial probe outlined in the previous section. As a result of increasing the cut angle of the aperture, (i.e., an increased sensing area), subsequently, an obvious greater contrast in │S₁₁│ and phase is achieved. In order to set a value of sample thickness for the sensitivity test with sharpest sensor, examination of the results in Figures 8 and 9 suggests it should be greater than 5 mm. The sensing distance is increased significantly from 0.64 mm for φ = 22.5° to 3 mm for φ = 80°, with increase ratio of about 369 %.
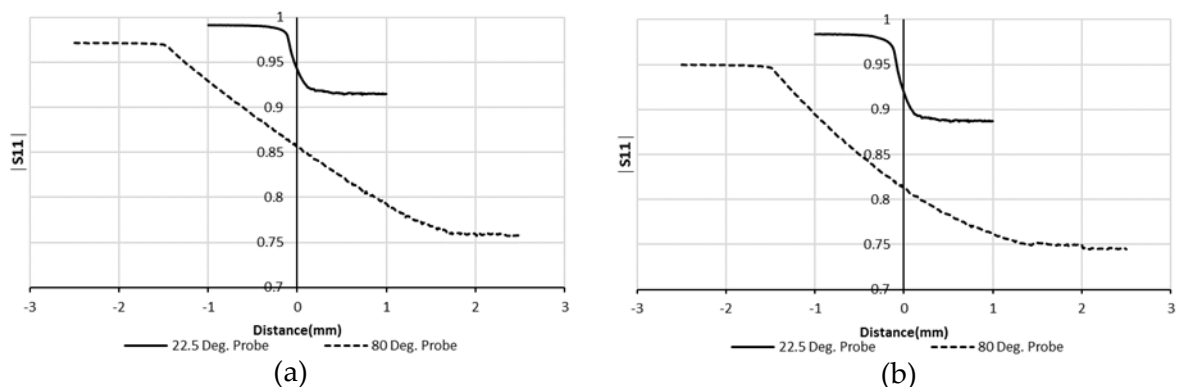

(a)   (b)

Figure 7: Magnitude of Reflection Coefficient of φ=22.5° and φ=80° sensors with distance for Fat and Muscle tissues at (a) 0.1 GHz, (b) 1 GHz.
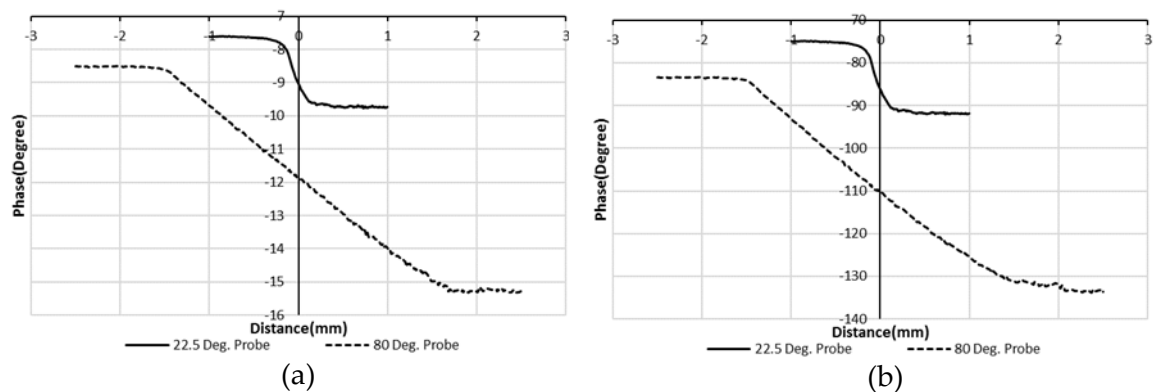
Figure 8: Phase of Reflection Coefficient of φ=22.5° and φ=80° sensors with distance for Fat and Muscle tissues at (a) 0.1 GHz, (b) 1 GHz.

5. Conclusions

It was shown that small dimensions open-ended elliptical coaxial sensors can be successfully made an obvious distinction between the phase and amplitude characteristics of the reflection coefficient for different values of the dielectric constant at frequency range of 0.1 GHz to 3 GHz. The key advantages of the $\varphi = 80°$ elliptic aperture sensor over the $\varphi = 22.5°$ aperture sensor are that as the cut aperture angle increases (i.e., sensing area increases), the measurement sensitivity increases. It is found that in the case $\varphi = 80°$, a contrast improvement of 193 % in $|S_{11}|$ and 218 % in phase may be achieved in comparison with the $\varphi = 22.5°$ sensor at 0.1 GHz. Furthermore, the elliptic sensor is suitable for future in vivo measurements of biological tissues due to its ease of insertion into living tissues.

References

[1]   Meaney, P.M., Gregory, A.P., Epstein, N.R. et al. Microwave open-ended coaxial dielectric probe: interpretation of the sensing volume re-visited. BMC Med Phys 14, 3 (2014).

[2]   Xu, G., Liu, H., Huang, Q. et al. Sensitivity investigation of open-ended coaxial probe in skin cancer detection. Phys Eng Sci Med (2023).

[3]   Xu, Y., F. M. Ghannouchi and R. G. Bosisio (1992). "Theoretical and experimental study of measurement of microwave permittivity using open ended elliptical coaxial probes." IEEE Transactions on Microwave Theory and Techniques 40(1): 143-150.

[4]   Xu, Y., R. Bosisio, A. Bonincontro, F. Pedone and G. F. Mariutti (1993). "On the measurement of microwave permittivity of biological samples using needle-type coaxial probes." IEEE Transactions on Instrumentation and Measurement 42(4): 822-827.

[5]   Athey, T. W., M. A. Stuchly and S. S. Stuchly (1982). "Measurement of Radio Frequency Permittivity of Biological Tissues with an Open-Ended Coaxial Line: Part I." IEEE Transactions on Microwave Theory and Techniques 30(1): 82-86.

[6]   Engelder, D. S. and C. R. Buffler (1991). "Measuring dielectric properties of food products at microwave frequencies." Microwave world 12(2): 6-15.

[7]   Langhe, P. D., K. Blomme, L. Martens and D. D. Zutter (1993). "Measurement of low-permittivity materials based on a spectral-domain analysis for the open-ended coaxial probe." IEEE Transactions on Instrumentation and Measurement 42(5): 879-886.

[8]   Gabriel, C. (1991). Permittivity Probe Modelling. King's College London.

[9]   Mosig, J. R., J. E. Besson, M. Gex-Fabry and F. E. Gardiol (1981). "Reflection of an open-ended coaxial line and application to nondestructive measurement of materials." IEEE Transactions on Instrumentation and Measurement IM-30(1): 46-51.

[10]   King, M. and J. Wiltse (1961). "Coaxial transmission lines of elliptical cross section." IRE Transactions on Antennas and Propagation 9(1): 116-118.

[11]   Keysight. (2010, Jul 13, 2010). " The Finite Element Method."   Retrieved September 22, 2022, from
https://edadocs.software.keysight.com/display/empro201101/Understanding+the+Process+of+FEM+Simulation.

[12]   Buckley, F. and A. A. Maryott (1958). Tables of Dielectric Dispersion Data for Pure Liquids and Dilute Solutions, U.S. Department of Comerce, National Bureau of Standards.